ELSEVIER

Journal of Organometallic Chemistry 659 (2002) 29–42

Journal of Organometallic Chemistry

www.elsevier.com/locate/jorganchem

Dehydrocoupling of tris(hydridosilylethyl)boranes and cyanamide: a novel access to boron-containing polysilylcarbodiimides

Markus Weinmann [a,*], Markus Hörz [a], Frank Berger [b], Anita Müller [a], Klaus Müller [b], Fritz Aldinger [a]

[a] *Max-Planck-Institut für Metallforschung and Institut für Nichtmetallische Anorganische Materialien, Pulvermetallurgisches Laboratorium, Universität Stuttgart, Heisenbergstr. 3, D-70569 Stuttgart, Germany*

[b] *Institut für Physikalische Chemie, Universität Stuttgart, Pfaffenwaldring 55, D-70569 Stuttgart, Germany*

Received 31 January 2002; received in revised form 20 May 2002; accepted 7 June 2002

In dedication to Professor Dr. Gottfried Huttner on the occasion of his 65th birthday

Abstract

The synthesis by a novel reaction pathway and the polymer-to-ceramic conversion of boron-containing polysilylcarbodiimides are reported. The title compounds are accessible by reaction of tris(hydridosilylethyl)boranes, $B[C_2H_4–Si(R)H_2]_3$ (R = H, CH_3; C_2H_4 = CH_2CH_2, $CHCH_3$) with different amounts of cyanamide, $H_2N–C{\equiv}N$, in tetrahydrofuran solution. Polymerization occurs by dehydrocoupling without the formation of solid by-products and without the use of catalysts. Overall compositions range from $C_{6.5}H_{20}BNSi_3$ to $C_9H_{15}BN_6Si_3$ in the case of the polymers obtained from $B(C_2H_4–SiH_3)_3$ and from $C_{9.5}H_{26}BNSi_3$ to $C_{12}H_{21}BN_6Si_3$ in the case of the polymers obtained from $B[C_2H_4–Si(CH_3)H_2]_3$, depending on the $B[C_2H_4–Si(R)H_2]_3$: $H_2N–C{\equiv}N$ ratio used. Molecular structure and chemical composition were investigated by spectroscopic methods (solid state MAS-NMR, FT-IR) and elemental analysis. Thermolysis in an Ar atmosphere delivers Si–B–C–N ceramics in 65–85% yield, depending on the elemental composition and the molecular structure, i.e. the cross-linking of the polymers.

Keywords: Cyanamide; Polysilylcarbodiimides; Tris(hydridosilylethyl)boranes; Preceramics

1. Introduction

Organometallic polymers based on silicon, boron, carbon, nitrogen, and hydrogen are precursors for Si–B–C–N ceramics [1–9]. These quaternary materials frequently possess extraordinary high temperature properties such as resistance towards thermal degradation, crystallization and oxidation. In general, the structural basis of the polymeric precursors are linear or cyclic silazanes, which are cross-linked via N–B–N [3], C–B–C [4,7], or $B(C_2–Si–C_2)_2$ units [9]. Alternatively, borazine-based oligosilazanes served for the synthesis of Si–B–C–N ceramics [1,5,6].

Recently, we described boron-modified polysilylcarbodiimides as novel precursors for Si–B–C–N ceramics [8]. Synthesis was performed on two different reaction pathways. In the first route vinyl-substituted polysilylcarbodiimides [8,10] were reacted with borane dimethyl sulfide according to Eq. (1):

* Corresponding author. Tel.: +49-711-6893231; fax: +49-711-6893131

E-mail address: weinmann@mf.mpg.de (M. Weinmann).

0022-328X/02/$ - see front matter
PII: S0022-328X(02)01668-6

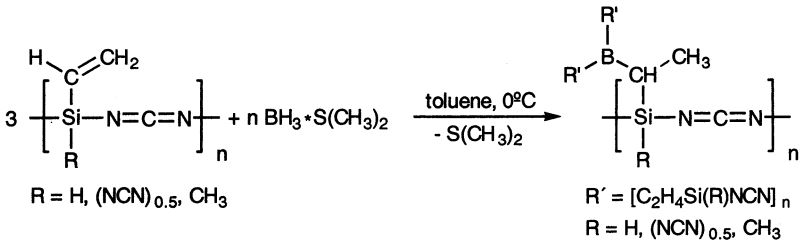

(1)

The second procedure, which delivered boron-modified polysilylcarbodiimides in a non-oxide sol–gel type reaction, is a *trans*-silylation reaction of tris(chlorosilylethyl)boranes [11] and excess bis(trimethylsilyl)carbodiimide (BTSC) which is represented in Eq. (2):

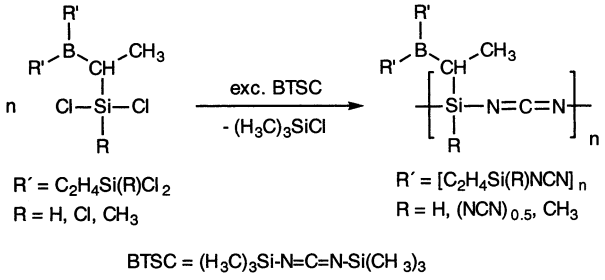

(2)

Both procedures occurred straight forwardly and delivered the precursors in high purity almost quantitatively.

The as-obtained polymers are suitable for producing bulk ceramic materials. Plastic forming of the boron-modified polysilylcarbodiimides at 120 °C/45 MPa and subsequent thermolysis of the obtained green bodies at 1400 °C yielded dense and crack-free ceramic monoliths which possessed less than 5% of open porosity [12].

In contrast to a couple of different Si–B–C–N materials obtained from boron-modified polysilazanes, however, ceramics derived from the above boron-modified polysilylcarbodiimides did not possess satisfactory high temperature properties. Thermally induced degradation already appeared at around 1550 °C, which is a value typical for ternary, boron-free Si–C–N ceramics [13]. Most probably, this decomposition is a consequence of a carbo-thermal reduction by the reaction of Si–N units of the predominantly amorphous material with free carbon upon which Si–C bonds form with the loss of molecular nitrogen [14].

Recently we have been able to demonstrate that thermal stability in polysilazane-derived Si–B–C–N ceramics strongly depends on the silicon nitride phase fraction, assuming that the materials are fully crystallized. On the basis of elemental analysis the phase composition in the ceramics was thermodynamically calculated by using the *CALPHAD* approach [15]. These calculations predicted SiC, Si_3N_4, and BN aside from 'free' carbon [7a,9a]. The amount of silicon nitride was depending on the Si–B–N ratio in the ceramic materials. This share was directly influenced by the chemical composition of the precursors. In the case of boron-modified polysilazanes of the general type $[B[C_2H_4–Si(R)NH]_3]_n$ the Si–B–N ratio was at 3:1:3 while polysilsesquiazane-type precursors $[B[C_2H_4–Si(NH)_{1.5}]_3]_n$ possessed a Si–B–N ratio of 3:1:4.5. Ceramics obtained from the first type of precursor resisted thermal decomposition up to 2000 °C whereas materials derived from the latter type decomposed at around 1500 °C. It is thus understandable that materials obtained from boron-modified polysilylcarbodiimides $[B[C_2H_4–Si(R)N=C=N]_3]_n$ also decomposed at relatively low temperature since the nitrogen content (Si–B–N ratio at 3:1:6 (R = H, alkyl) or 3:1:9 (R = $(N=C=N)_{0.5}$)) in these precursors was even higher than in boron-substituted polysilsesquiazanes.

The main intention of this study is to report on a procedure, which allows for the synthesis of boron-modified polysilylcarbodiimides with adjustable nitrogen content. Until now, synthesis of polysilylcarbodiimides was performed by either metathesis reactions with formation of salts [16] or by the above mentioned *trans*-silylation reactions [17]. None of these methods allows for the synthesis of polysilylcarbodiimides with low nitrogen concentration. In contrast to these procedures we here describe a novel reaction sequence, in which tris(hydridosilylethyl)boranes are dehydro-coupled with cyanamide. Using this procedure, synthesis of boron-modified polysilylcarbodiimides with Si–N atomic ratios ranging from 3:1 to 3:6 is possible.

2. Results and discussion

2.1. Synthesis

Boron-modified silylcarbodiimides $[[H_2(R)Si–C_2H_4]_2B[C_2H_4–Si(R)H(N=C=N)_{0.5}]]_2$ (R = H, CH_3; **R–N1**) and polysilylcarbodiimides of the general types $[B[C_2H_4–Si(R)H(N=C=N)_{0.5}]_2[C_2H_4–Si(R)H_2]]_n$ (R = H, CH_3; **R–N2**) and $[B[C_2H_4–Si(R)N=C=N]_x[C_2H_4–Si(R)H(N=C=N)_{0.5}]_{3-x}]_n$ (R = H, CH_3; $x = 0$: **R–N3**,

$x = 1$: **R**–**N4**, $x = 2$: **R**–**N5**, $x = 3$: **R**–**N6**) were obtained by a dehydrocoupling reaction of tris(hydridosilylethyl)boranes, $B[C_2H_4–Si(R)H_2]_3$ ($R = H$, CH_3), with cyanamide, $H_2N–C{\equiv}N$. The synthesis of tris(hydridosilylethyl)boranes by two independent reaction pathways was published recently. Here, we chose in-situ hydroboration of vinylsilanes with borane dimethyl sulfide in toluene solution as pointed out in Eq. (3) [18]:

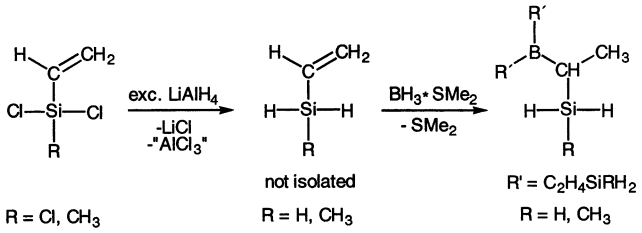

(3)

The hydroboration is not regioselective, rather the boryl group may add in each of the three successive hydroboration steps at either the 1- or 2-position of the vinyl function whereby a mixture of regio- and diastereomers is obtained. For the purpose of this work, a separation of the different regio- and diastereomers that form upon hydroboration was not achieved.

Dehydrocoupling was performed in a one-pot-reaction by dissolving cyanamide in tetrahydrofuran and subsequent mixing with different amounts of the silanes. A catalyst as required for the dehydrocoupling of tris(hydridosilylethyl)boranes and ammonia or amines that we described previously [19] was not used. Under vigorous stirring, the reaction solutions were refluxed for 12 h. Strong hydrogen evolution and precipitation of the precursors occurred thereby. In the case of the more highly cross-linked precursors **H**–**N4**, **H**–**N5** and **H**–**N6** and **Me**–**N4**, **H**–**N5** and **Me**–**N6** the reaction mixtures gelled within 30–120 min.

After cooling to room temperature, all volatile components were removed at 25 °C/10^{-1} mbar. The colorless precipitates were carefully rinsed twice with each 100 ml of diethyl ether and finally dried at 130 °C/10^{-2} mbar to deliver boron-modified polysilylcarbodiimides as colorless very air- and moisture-sensitive powders.

The molar ratio of the starting compounds $B[C_2H_4–Si(R)H_2]_3$ and cyanamide ranged from 1:0.5 to 1:3 as shown in reaction scheme (4). The terms, which will further be used to distinguish the different compounds are the following: **H** and **Me** differentiate between polymers derived from $B[C_2H_4–SiH_3]_3$ and $B[C_2H_4–Si(CH_3)H_2]_3$, respectively, whereas the indexes **N1**–**N6** specify the numbers of nitrogen atoms per boron atom (for details see Tables 1 and 2). Additionally, derivatives **N3.5**, **N4**, and **N5**, which are not depicted in Scheme (4),

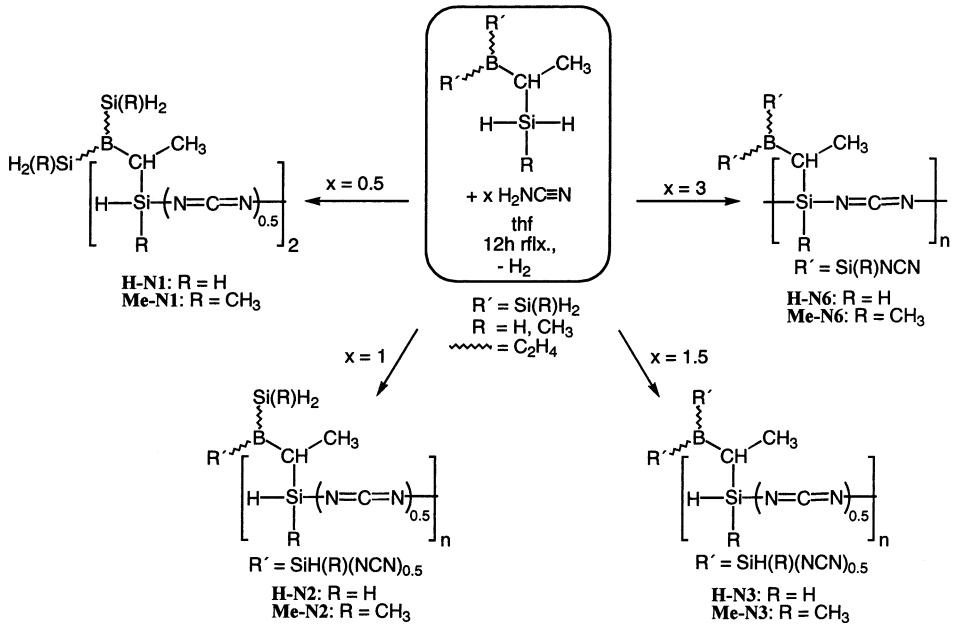

(4)

were synthesized.

H–**N1** and **Me**–**N1** are monomeric species in which two $[H_2(R)Si–C_2H_4]_2B[C_2H_4–Si(R)H]$ groups are

Table 1
Idealized structure and sum formulas of boron-modified silylcarbodiimide **H–N1** and polysilylcarbodiimides **H–N2**–**H–N6** obtained from $B(C_2H_4–SiH_3)_3$ and $H_2N–C{\equiv}N$

	Silane–cyanamide	Idealized structure (monomer unit)	Sum formula (momomer unit)
H–N1	1:0.5	$B[C_2H_4–SiH_2–(N=C=N)_{0.5}][C_2H_4–SiH_3]_2$	$C_{6.5}H_{20}BNSi_3$
H–N2	1:1	$B[C_2H_4–SiH_2–(N=C=N)_{0.5}]_2[C_2H_4–SiH_3]$	$C_7H_{19}BN_2Si_3$
H–N3	1:1.5	$B[C_2H_4–SiH_2–(N=C=N)_{0.5}]_3$	$C_{7.5}H_{18}BN_3Si_3$
H–N4	1:2	$B[C_2H_4–SiH–N=C=N][C_2H_4–SiH_2–(N=C=N)_{0.5}]_2$	$C_8H_{17}BN_4Si_3$
H–N5	1:2.5	$B[C_2H_4–SiH–N=C=N]_2[C_2H_4–SiH_2–(N=C=N)_{0.5}]$	$C_{8.5}H_{16}BN_5Si_3$
H–N6	1:3	$B[C_2H_4–SiH–N=C=N]_3$	$C_9H_{15}BN_6Si_3$

Table 2
Idealized structure and sum formulas of boron-modified silylcarbodiimide **Me–N1** and polysilylcarbodiimides **Me–N2**–**Me–N6** obtained from $B[C_2H_4–Si(CH_3)H_2]_3$ and $H_2N–C{\equiv}N$ ($Me{=}CH_3$)

	Silane–cyanamide	Idealized structure (monomer unit)	Sum formula (momomer unit)
Me–N1	1:0.5	$B[C_2H_4–SiMeH–(N=C=N)_{0.5}][C_2H_4–SiMeH_2]_2$	$C_{9.5}H_{26}BNSi_3$
Me–N2	1:1	$B[C_2H_4–SiMeH–(N=C=N)_{0.5}]_2[C_2H_4–SiMeH_2]$	$C_{10}H_{25}BN_2Si_3$
Me–N3	1:1.5	$B[C_2H_4–SiMeH–(N=C=N)_{0.5}]_3$	$C_{10.5}H_{24}BN_3Si_3$
Me–N4	1:2	$B[C_2H_4–SiMe–N=C=N][C_2H_4–SiMeH–(N=C=N)_{0.5}]_2$	$C_{11}H_{23}BN_4Si_3$
Me–N5	1:2.5	$B[C_2H_4–SiMe–N=C=N]_2[C_2H_4–SiMeH–(N=C=N)_{0.5}]$	$C_{11.5}H_{22}BN_5Si_3$
Me–N6	1:3	$B[C_2H_4–SiMe–N=C=N]_3$	$C_{12}H_{21}BN_6Si_3$

linked by a carbodiimide unit, whereas **H–N2** and **Me–N2** are linear polymers or cyclic oligomers. In the latter compounds two of the three silicon-containing groups of the starting compounds constitute the polymer backbone; the third $C_2H_4–Si(R)H_2$-unit remains as a side arm. **H–N3** and **Me–N3** are polymers in which one silicon-bonded hydrogen atom of each of the $C_2H_4Si(R)H_2$-units of the starting compounds is replaced by a carbodiimide group. The polymer skeleton is thus composed of $[C_2H_4–Si(R)H]_2N{=}C{=}N$ blocks, which are cross-linked via boron atoms. **H–N6** and **Me–N6** are most highly cross-linked. In these compounds, a second silicon-bonded hydrogen atom is substituted by a $N{=}C{=}N$ unit. Details on the stoichiometry and idealized chemical compositions of all synthesized polymers are given in Tables 1 and 2.

The novel precursors are colorless solids, which are poorly soluble in common organic solvents (**H–N1**, **Me–N1**) or which are insoluble (**H–N2** to **H–N6**, **Me–N2** to **Me–N6**). Their structural characterization was performed by solid state NMR and FT-IR spectroscopy. Molecular weight determinations could not be achieved because of to the insolubility of the polymers. Chemical compositions were determined by elemental analysis using a combination of combustion methods and atom emission spectrometry. For details, compare Tables 3 and 4 and general comments in the experimental section (4.1).

It is evident from Tables 3 and 4 that found and calculated elemental compositions of the precursors are in a good agreement. A deviation, however, is observed for **H–N1** and **Me–N1**. In these compounds, the

Table 3
Found and calculated (in italics) elemental composition (mass %) of **H–N1**–**H–N6**

	H–N1	**H–N2**	**H–N3**	**H–N3.5**	**H–N4**	**H–N5**	**H–N6**
C	36.3	36.9	33.3	37.3	38.4	37.8	38.3
	37.66	*37.15*	*36.72*	*36.53*	*36.36*	*36.04*	*35.76*
H	8.2	7.3	7.2	7.1	7.1	6.4	5.5
	9.72	*8.46*	*7.40*	*6.92*	*6.48*	*5.69*	*5.00*
N	10.2	14.5	18.6	19.7	20.8	22.8	27.0
	6.75	*12.37*	*17.12*	*19.23*	*21.19*	*24.71*	*27.79*
Si	35.1	36.9	33.3	32.0	30.0	29.7	26.0
	40.65	*37.24*	*34.35*	*33.07*	*31.88*	*29.74*	*27.87*
B	4.8	4.4	4.2	3.9	3.7	3.3	3.2
	5.22	*4.78*	*4.41*	*4.25*	*4.09*	*3.82*	*3.58*

Table 4
Found and calculated (in italics) elemental composition (mass %) of **Me–N1**–**Me–N6**

	Me–N1	**Me–N2**	**Me–N3**	**Me–3.5**	**Me–N4**	**Me–N5**	**Me–N6**
C	42.7	44.1	43.2	42.9	42.5	42.2	41.3
	45.75	*44.75*	*43.88*	*43.49*	*43.12*	*42.45*	*41.85*
H	8.1	9.0	8.1	8.0	8.1	7.8	6.9
	10.51	9.39	*8.42*	*7.98*	*7.57*	*6.82*	*6.15*
N	13.6	13.5	16.3	16.3	17.9	19.4	23.2
	5.611	*10.43*	*14.62*	*16.51*	*18.28*	*21.51*	*24.39*
Si	31.4	29.6	28.6	29.5	26.3	22.7	25.8
	33.79	*31.40*	*29.32*	*28.38*	*27.50*	*25.90*	*24.47*
B	4.2	3.8	3.8	3.3	3.5	3.1	2.8
	4.34	*4.03*	*3.76*	*3.64*	*3.53*	*3.32*	*3.14*

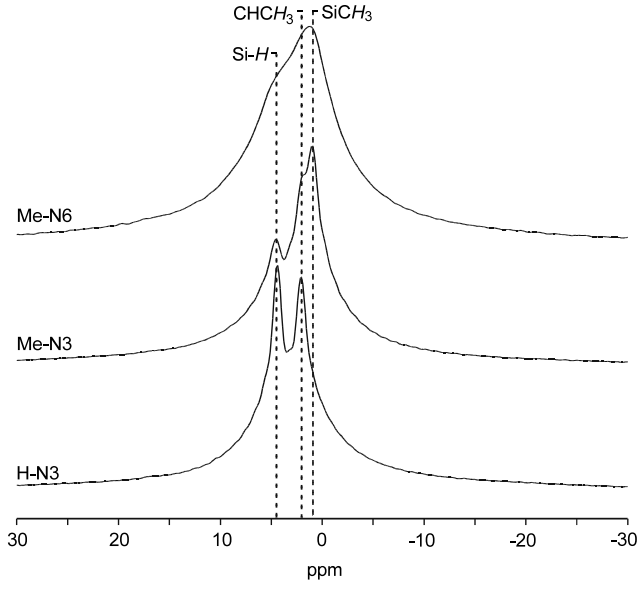

Fig. 1. ^{1}H MAS-NMR spectra of **H–N3**, **Me–N3** and **Me–N6** recorded at 300.13 MHz, sample rotation frequency 12 kHz.

nitrogen values are significantly too high, whereas the concentration of all other elements is too low. This is probably a consequence of the reaction conditions chosen: **H–N1** and **Me–N1** are mixed with cyanamide at room temperature. Dehydrocoupling occurs spontaneously without pronounced selectivity. As a consequence, there is more than one of the three boron-bonded C_2H_4–$SiRH_2$ units per $B[C_2H_4–Si(R)H_2]_3$ molecule involved in dehydrocoupling reactions. Accordingly, also higher cross-linked species form, whereas corresponding amount of the starting compound $B[C_2H_4–Si(R)H_2]_3$ remains unreacted. The latter evaporates during the work-up of the reaction mixture and causes the low determination of hydrogen, boron, carbon, and silicon compared to the calculated values.

2.2. NMR spectroscopy

Except ^{15}N whose natural abundance is too low for obtaining sufficient signal-to-noise ratio, the isotopes ^{1}H, ^{11}B, ^{13}C, and ^{29}Si, which constitute the title compounds, are suitable for performing NMR investigations. Because of the insolubility of the precursors in organic solvents, solid state MAS-NMR investigations had to be performed. In contrast to high resolution NMR spectroscopy in solution, resonance signals in these spectra appear remarkably broadened. It is thus difficult to structurally unequivocally assign and distinguish between different structural motifs present in the polymers.

The main features in the starting compounds $B[C_2H_4–Si(R)H_2]_3$ and $H_2N–C{\equiv}N$ which were considered to obtain information on the molecular structures of the polymers are N–H, C≡N and Si–H units that disappear/remain as well as Si–N=C=N units that form upon the dehydrocoupling. In the following, the results of ^{1}H-, ^{13}C-, ^{11}B- and ^{29}Si MAS-NMR will be discussed and finally molecular structures be suggested.

The resonance signals in the proton NMR spectra of all precursors appear broadened without fine structure and significantly overlap. As an example, the ^{1}H-NMR spectra of **H–N3**, **Me–N3** and **Me–N6** are depicted in Fig. 1.

The spectrum of **H–N3** possesses two resonance signals at around 2.0 and 4.5 ppm, which can be attributed to $CHCH_3$ and SiH_2 protons, respectively. Their intensities are similar, which is in accordance with the proposed composition, presuming α:β-hydroboration in the synthesis of $B[C_2H_4–SiH_3]_3$ occurred in a ca. 3:1 ratio, as described in the literature [18]. A very weak shoulder at 2.7 ppm points to CH and CH_2 protons of the C_2H_4 unit ($C_2H_4 = CHCH_3$, CH_2CH_2). The ^{1}H-NMR spectrum of **Me–N3** appears comparably, except that due to the presence of Si–CH_3 protons an additional resonance signal at ca. 1.0 ppm is generated. As expected, the intensity of the Si–H resonance signal is

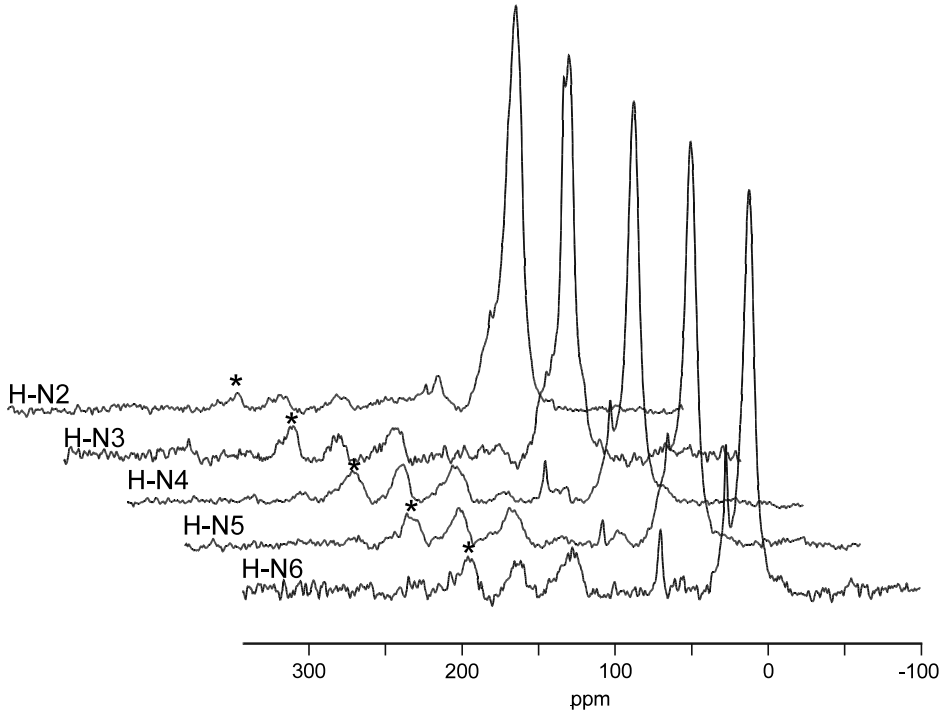

Fig. 2. ^{13}C CP-MAS-NMR spectra of **H**–**N2**–**H**–**N6** recorded at 75.47 MHz, sample rotation frequency 5 kHz; the signals marked with an asterisk at ca. 195 ppm are spinning side bands.

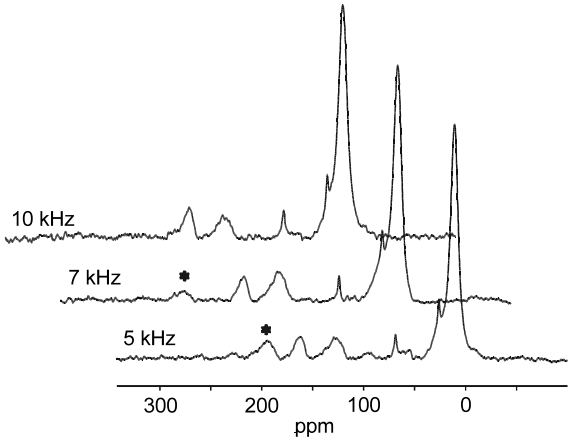

Fig. 3. ^{13}C CP-MAS-NMR spectra of **H**–**N4** recorded at 75.47 MHz with different sample rotation frequencies: 5, 7, and 10 kHz.

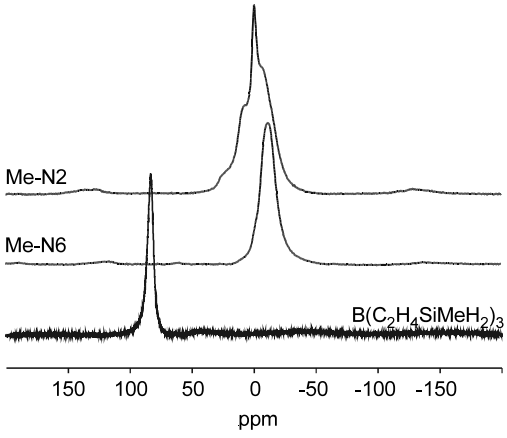

Fig. 4. ^{11}B MAS-NMR spectra of **Me**–**N2** and **Me**–**N6** recorded at 96.29 MHz (sample rotation frequency 12 kHz) and $^{11}B\{^1H\}$-NMR spectrum of $B[C_2H_4–Si(CH_3)H_2]_3$ recorded at 80.24 MHz in C_6D_6 solution.

significantly lower than in the spectrum of **H**–**N3**. The spectrum of **Me**–**N6**, in contrast, is dominated by a broad resonance signal which stretches over several ppm and which is centered at ca. 1 ppm. The significant line broadening is a consequence of the high cross-linking of this compound. A shoulder at 4.5 ppm points to residual silicon-bonded protons, indicating the dehydrocoupling did not proceed quantitatively.

The ^{13}C MAS-NMR spectra of the title compounds are characterized by the appearance of resonance signals at around 0 ppm (only **Me**–**N1** to **Me**–**N6**), 10–25 ppm and 125 ppm. They are generated by silicon-bonded methyl groups (only **Me**–**N** polymers), aliphatic C-atoms of the $B–C_2H_4–Si$ units and carbodiimide C-atoms, respectively. As an example, the spectra of **H**–**N2** to **H**–**N6**, which are depicted in Fig. 2 as a staggered plot, are discussed in more detail. Resonance signals of $CHCH_3$ C-atoms are found at ca. 10 ppm. CH_2 and CH signals in all polymers emerge as a shoulder of the $CHCH_3$ resonance. The resonance of the carbodiimide C-atoms is observed at 125–130 ppm. The intensity of this signal compared to CH_3 increases with increasing nitrogen content of the polymers. Moreover, two

additional low-field shifted signals centered at 165 and 195 ppm are observed. As shown in Fig. 3 for **H–N4**, the latter is a spinning side band which shifts to 225 ppm if the spinning rate is increased from 5 to 7 kHz and which disappears if the rotation frequency is further increased to 10 kHz.

A possible explanation for the presence of the resonance signals at 165 ppm is an interaction of the electron lone pairs of the carbodiimide N-atoms with the boron centers. Because of this coordination, the C-atom is de-shielded and its resonance shifted to lower field. This assumption is further supported by observations in the ^{11}B MAS-NMR and FT-IR spectra which are discussed below in more detail. In addition to the product signals, further signals at 28 and 70 ppm arise in the case of the highly cross-linked precursors. These are generated by residual tetrahydrofuran which was used as a solvent in the synthesis of the title compounds. Most probably the solvent was encapsulated in the porous gel that formed during the reaction. As an inclusion within the gel, it could not be eliminated quantitatively in the final drying step. The ^{13}C MAS-NMR spectra of **Me–N2** to **Me–N6** are very comparable with those of **H–N2** to **H–N6**, the only significant difference is the additional appearance of Si*C*H$_3$ resonance signals at ca. 0 ppm.

Compared to the ^{11}B{^{1}H}-NMR signal of the starting compound B[C$_2$H$_4$–Si(CH$_3$)H$_2$]$_3$ (recorded in C$_6$D$_6$ solution; Fig. 4), the ^{11}B MAS-NMR spectra of the title compounds all show very broad resonance signals which are located between 0 and −10 ppm. Both the chemical shift and the multiplicity, i.e. the lack of a quadrupolar coupling, point to a (distorted) tetrahedral environment of the boron atoms in the solid state, most likely due to their interaction with the electron lone pairs of carbodiimide units, as already discussed above. By a comparison of the ^{11}B MAS-NMR spectra of **Me–N2** and **Me–N6** (Fig. 4) it can be concluded that the amount of

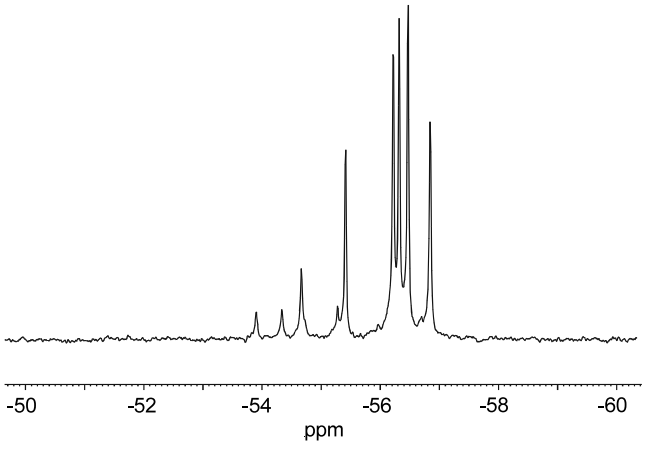

Fig. 5. ^{29}Si{^{1}H}-NMR (49.692 MHz) of B[C$_2$H$_4$–SiH$_3$]$_3$ (0.2 M in C$_6$D$_6$) obtained from (H$_2$C=CH)SiH$_3$ and BH$_3$·S(CH$_3$)$_2$.

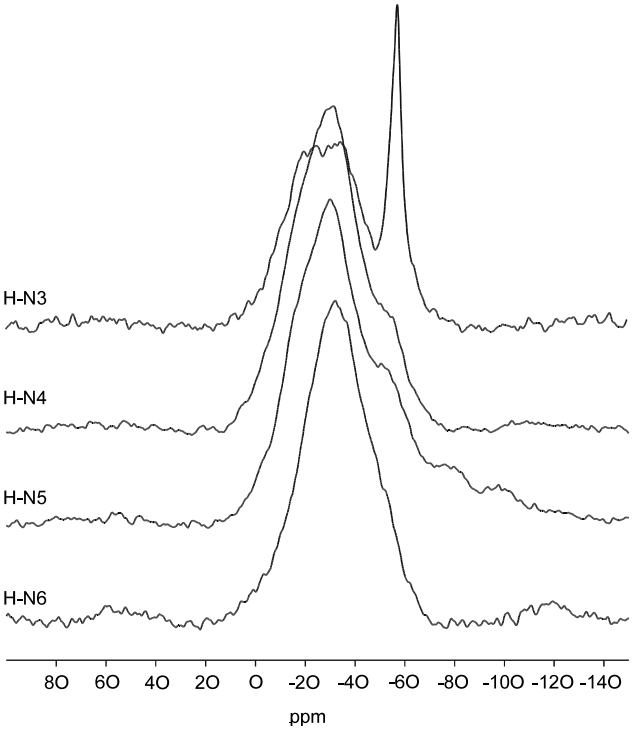

Fig. 6. ^{29}Si CP-MAS-NMR spectra of **H–N3**–**H–N6** recorded at 59.60 MHz, sample rotation frequency 5 kHz.

nitrogen present in the precursors influences signal appearance and chemical shift values substantially.

Obviously, the boron atoms in **Me–N2** do not possess a homogeneous (tetrahedral) environment, since the ^{11}B-NMR spectrum displays a resonance signal centered at 0 ppm, which exhibits shoulders at 20, 5, and −5 ppm. Possible reasons therefore are the lacking selectivity of the dehydrocoupling, resulting in a mixture of B[C$_2$H$_4$–Si(CH$_3$)H–(N=C=N)$_{0.5}$]$_n$[C$_2$H$_4$–Si(CH$_3$)H$_2$]$_{3-n}$ sites. In contrast, the spectrum of **Me–N6** possesses only one sharp resonance signal at −10 ppm. The spectra of **Me–N3**, **Me–N4** and **Me–N5** appear in between these extremes. A similar trend is observed for **H–N2** to **H–N6**: with increasing nitrogen content the resonance signals are shifted towards higher field and the line width decreases in this row.

^{29}Si MAS-NMR spectroscopy is an ideal tool to investigate the progress in the dehydrocoupling of B[C$_2$H$_4$–Si(R)H$_2$]$_3$ and H$_2$N–C≡N. The substitution of a silicon-bonded hydrogen atom by a carbodiimide unit results in a low field shift of the ^{29}Si resonance signals.

As an example, the ^{29}Si-NMR spectra of **H–N3** to **H–N6** are displayed in Fig. 6 and compared with the ^{29}Si{^{1}H}-NMR spectrum of the starting compound B[C$_2$H$_4$–SiH$_3$]$_3$, which was recorded in C$_6$D$_6$ solution and which is shown in Fig. 5.

As a consequence of the lack of regioselectivity in the hydroboration of (H$_2$C=CH)SiH$_3$ using borane di-

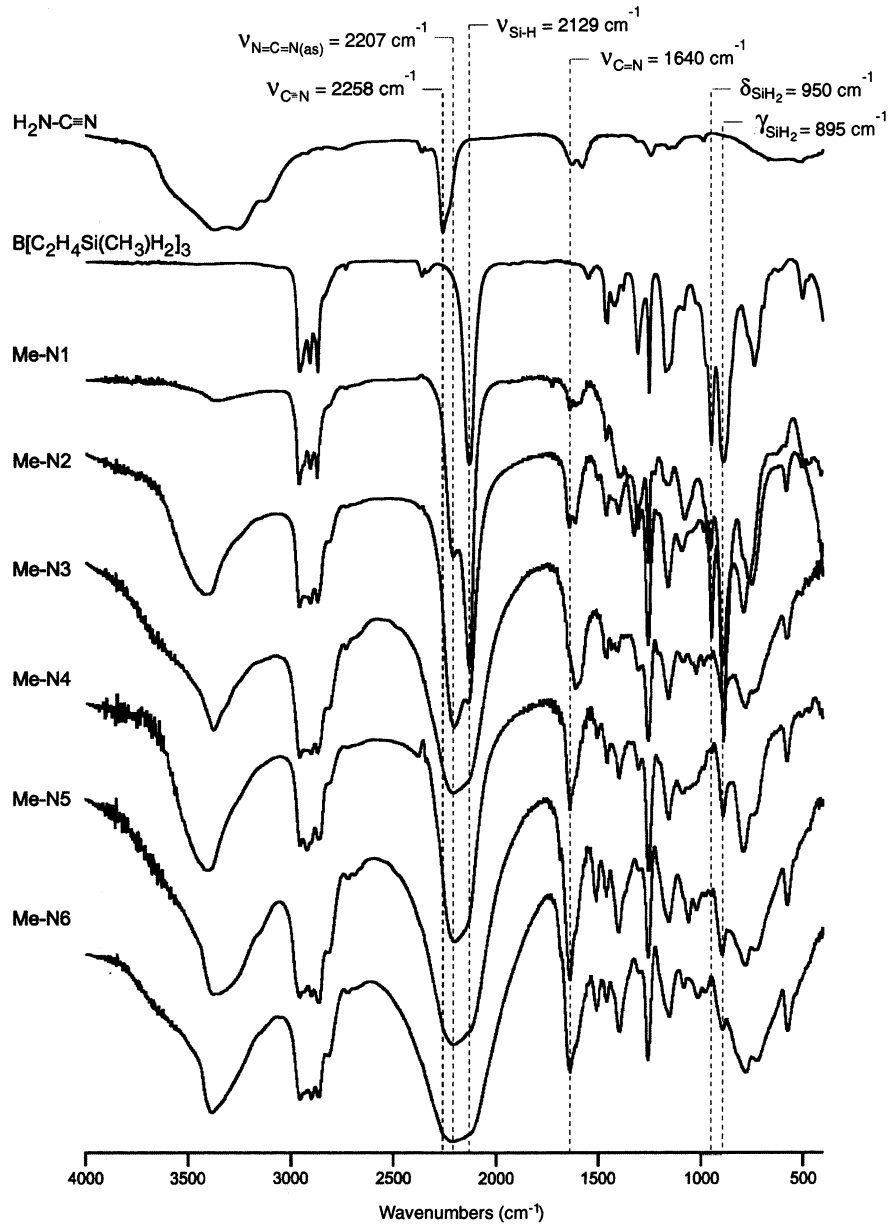

Fig. 7. FT-IR spectra of **Me**–**N1**–**Me**–**N6** and the starting compounds cyanamide, $H_2NC{\equiv}N$, and $B[C_2H_4Si(CH_3)H_2]_3$.

methyl sulfide, a mixture of regio- and diastereomers is obtained, which causes the formation of a set of nine resonance signals which appear between −54 and −57 ppm. However, in the solid state NMR spectra, these cannot be distinguished, since a significant line broadening causes an overlap of these resonances.

The above discussed lack of selectivity of the dehydrocoupling of $B[C_2H_4–Si(R)H_2]_3$ and $H_2N–C{\equiv}N$ is mirrored in the ^{29}Si MAS-NMR spectrum of **H**–**N3**. Apart from a broadened signal which is an overlap of two resonance signals at −18 and −28 ppm and which corresponds to a mixture of $CSiH_2(NCN)$ and $CSiH(NCN)_2$ environments (these obviously appear in a nearly identical chemical shift range), there is an intensive signal observed, centered at −57 ppm. The latter can be assigned unequivocally to residual $CSiH_3$ motifs in the polymer (compare Fig. 5). However, the intensity of the latter tremendously decreases in **H**–**N4** and **H**–**N5** whereas it is completely absent in **H**–**N6**. Moreover, the product signals change their appearance. In **H**–**N4**, **H**–**N5** and **H**–**N6**, only one broad signal at −32 ppm is observed.

Identical observations are made in the ^{29}Si MAS-NMR spectra of the methyl-substituted derivatives **Me**–**N2** to **Me**–**N6** which are not shown here. **Me**–**N2** and **Me**–**N3** each display a set of three resonance signals centered at −2, −12, and −30 ppm. The latter is again generated by residual C_2SiH_2 motifs, whereas the

former correspond to $C_2SiH(NCN)$ and $C_2Si(NCN)_2$ environments. In the NMR spectra of **Me–N4**, **Me–N5** and **Me–N6**, in contrast, the high field signal is totally absent.

2.3. IR and Raman spectroscopy

IR spectroscopy is the second spectroscopic tool to investigate the progress in the dehydrocoupling of tris(hydridosilylethyl)boranes $B[C_2H_4–Si(R)H_2]_3$ and cyanamide. In the following, only the IR spectra of the methyl-substituted derivatives **Me–N1** to **Me–N6** obtained from $B[C_2H_4Si(CH_3)H_2]_3$ will be discussed in more detail. The results obtained for **H–N1** to **H–N6** are almost identical. Spectroscopic details are available in Section 4.

Fig. 7 shows IR spectra of **Me–N1** to **Me–N6** as a staggered plot. For comparison, the IR spectra of the starting compounds cyanamide and $B[C_2H_4–Si(CH_3)H_2]_3$ are added. The most characteristic features in the spectrum of cyanamide are an intensive signal at 2258 cm^{-1} which is caused by an absorption due to $\nu(C\equiv N)$ vibrations and broad $\nu(N–H)$ absorptions at around 3270 and 3405 cm^{-1}. In contrast, a very strong absorption signal at 2129 cm^{-1} in $B[C_2H_4–Si(CH_3)H_2]_3$, which corresponds to a Si–H stretching and two strong signals at 950 and 895 cm^{-1}, generated by $\delta(SiH_2)$ and $\gamma(SiH_2)$ (wagging), are especially considered in the discussion of the progress of the dehydrocoupling. From Fig. 7 it is evident that the latter signals are most intensive in the starting compound $B[C_2H_4–Si(CH_3)H_2]_3$. They both decrease in intensity in **Me–N1** and **Me–N2** and vanish in **Me–N3** to **Me–N6** which is in accordance with the proposed structure of the more highly cross-linked polymers. On the other hand, the substitution of one hydrogen atom in $B[C_2H_4–Si(CH_3)H_2]_3$ with a N=C=N unit in the synthesis of **Me–N1** results in the appearance of an absorption at 2207 cm^{-1} which can be traced back to ν_{as}(N=C=N) and which is observed as a shoulder of ν(Si–H). In comparison to $B[C_2H_4–Si(CH_3)H_2]_3$, the latter signal is insignificantly blue shifted. Compared to **Me–N1** the signal intensities of ν_{as}(N=C=N) and ν(Si–H) are inverted in **Me–N2** in which ν(Si–H) is now observed as a shoulder of the former mentioned vibration. In **Me–N3** to **M–N6** ν_{as}(N=C=N) and ν(Si–H) cannot be distinguished any more since the line width of the dominant N=C=N stretching band, which is in all polymers centered at around 2200 wave numbers, considerably increases thus masking Si–H vibration bands. However, ν_{as}(N=C=N) and ν(Si–H) can be distinguished by combining Raman and IR spectroscopy as shown in Fig. 8 for **H–N3**.

In contrast to IR spectroscopy ν_{as}(N=C=N) is Raman forbidden. This allows for a clear assignment of Si–H functions present in the polymeric precursors. In addition to the Si–H stretching at 2147 cm^{-1}, scattering signals at 2929, 2868, as well as 1460 cm^{-1} are found in the Raman spectrum of **H–N3**. The first signals correspond to C–H vibrations, whereas the second scattering signal cannot be assigned unequivocally. Most probably, it relates to ν_s(N=C=N). Raman spectrum of boron-free polysilylcarbodiimide $[Me-Si(NCN)_{1.5}]_n$, which was described in the literature by Riedel and co-workers [20], appeared similarly, even though in comparison with **H–N3** signals were found red-shifted by ca. 60 cm^{-1} at 2974, 2906, and 1533 cm^{-1}.

Moreover, FT-IR spectroscopy supports the above assumption that carbodiimide units interact with boron atoms in the precursors by the appearance of a new absorption signal that evolves in spectra of all polymers

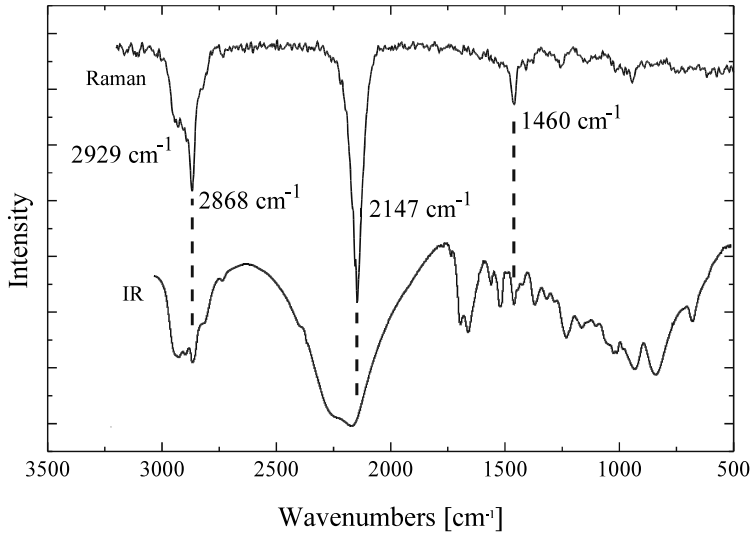

Fig. 8. Raman (top) and FT-IR spectra of **H–N3**.

at around 1640 cm^{-1}. Its intensity increases with increasing amount of cyanamide used in the dehydrocoupling. We suspect that it refers to ν(C=N) which would be in accordance with the observation of a broad resonance signals observed in all ^{13}C MAS-NMR spectra at ca. 160 ppm and which could be explained by an interaction of the electron lone pairs of the nitrogen atom or π-electrons of carbodiimide units with the boron centers:

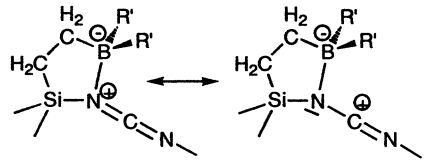

(5a)

or

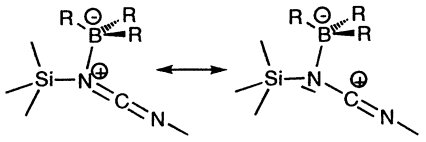

(5b)

This suggestion was already made above in the discussion of the ^{11}B MAS-NMR spectra of the title compounds: due to the transformation of the trigonal planar coordination sphere of the boron centers in the starting compounds into a distorted tetrahedral environment, resonance signals of the polymers are high field shifted to 0–10 ppm compared to that of $B[C_2H_4–Si(CH_3)H_2]_3$ ($\delta = 85$ ppm). However, it is not yet clear whether the interaction proceeds intramolecularly as shown in Scheme (5a) for a β-hydroboration product or via an intermolecular coordination of 'close-by' boron atoms and carbodiimide units as shown in Fig. 5b.

In addition, a number of absorption signals such as ν(C–H) at around 2860–2970 cm^{-1}, δ_a(C–CH_3) at ca. 1480 cm^{-1}, δ_s(C–CH_3) at ca. 1400 cm^{-1}, and δ_a(Si–CH_3) at ca. 1250 cm^{-1} which are present in $B[C_2H_4–Si(CH_3)H_2]_3$ are maintained in all polymers.

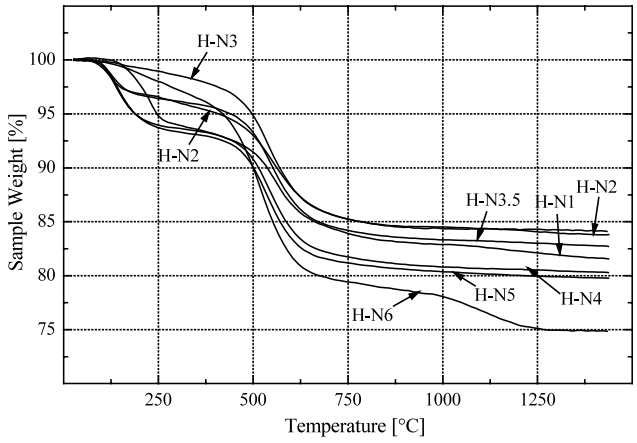

Fig. 9. TGA of **H**–**N1**–**H**–**N6**; heating rate 5 °C min^{-1}, flowing Ar (50 ml min^{-1}).

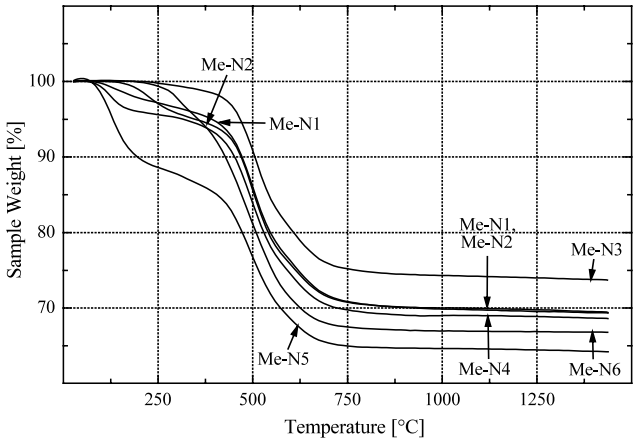

Fig. 10. TGA of **Me**–**N1**–**Me**–**N6**; heating rate 5 °C min^{-1}, flowing Ar (50 ml min^{-1}).

2.4. Thermogravimetric analysis

The thermally induced polymer-to-ceramic conversion of organometallic polymers into ceramic materials is always accompanied by the formation of volatile by-products which cause a mass loss upon the heat treatment. In this regard, the ceramic yield, which is the share of $(m_{ceramic}/m_{precursor}) \times 100\%$ is a subject of major importance in that it proves the general applicability of an organoelement polymer as a preceramic material. A common method for monitoring the progress during thermolysis and for determining ceramic yields is simultaneous thermogravimetric analysis (TGA). Figs. 9 and 10 show the results of the TGA of **H**–**N1** to **H**–**N6** and **Me**–**N1** to **Me**–**N6**, respectively. All measurements were performed in a flowing atmosphere of purified Ar (50 ml min^{-1}) in a temperature range of 25–1400 °C using a heating rate of 5 °C min^{-1}.

Thermolysis of **H**–**N1** to **H**–**N6** (Fig. 9) delivers ceramics in 75–84% yield, depending on the molecular structure, i.e. the degree of cross-linking. Surprisingly, the polymers with the lowest degree of cross-linking **H**–**N2** and **H**–**N3** have the highest ceramic yields at ca. 84%. The more highly cross-linked precursors **H**–**N4** and **H**–**N5** deliver ceramics in 81 and 80% yield, respectively, whereas the most highly cross-linked precursor **H**–**N6** delivers ceramics in 75% yield. To confirm this series, TGA of an additional precursor, **H**–**N3.5** (83% ceramic yield) which is not discussed here in more detail, was considered.

These unusual results indicate that not only high cross-linking is a prerequisite for a high yield polymer-to-ceramic conversion of boron-modified polysilylcarbodiimides. An other important issue is sufficient latent reactivity of the precursors, i.e. the ability to undergo cross-linking reactions during the heat treatment, most probably due to Si–H addition (hydrosilylation) to the

N=C=N units. This argument is especially valid for **H–N1** which—even though it is a monomer—delivers ceramics in 82% yield. Detailed investigations by means of MAS-NMR and IR spectroscopy of the intermediates that form during thermolysis are in progress and will be published soon [21].

The ceramic yields of **Me–N1** to **Me–N6** obtained from $B[C_2H_4–Si(CH_3)H_2]_3$ are in between 65 and 74% and thus ca. 10% lower than those obtained from **H–N1** to **H–N6**. This is mainly a consequence of the methyl group, which is bonded to the silicon centers. In contrast to the silicon bonded hydrogen atoms, this unit is not able to undergo cross-linking reactions such as thermally induced hydrosilylation. The tendency that ceramic yields increase with decreasing amount of cyanamide as observed for the **H–N1** to **H–N6** series is also valid for the methyl-substituted derivatives though with slight exceptions. **Me–N3** has the highest ceramic yield at 74%, whereas **Me–N1** and **Me–N2** deliver ceramics in 70% yield. These values subside to 69, 67, and 64% for **Me–N4**, **Me–N6**, and **Me–N5**.

However, the progress during thermolysis in both systems is very similar. It is characterized by a one step (**H–N3**, **H–N6**, **Me–N3**, **Me–N6**,) or two step decomposition. In all cases with exception of **H–N1** and **H–N6** thermolysis is completed at 750 °C. In the case of **H–N1** an insignificant mass loss of ca. 1% occurs between 1100 and 1400 °C, which is most probably due to hydrogen elimination, whereas in the case of **H–N6** a mass loss of 3% is observed in the 900–1250 °C range, which is due to elimination of cyanogen and nitrogen.

3. Conclusion and outlook

Dehydrogenative coupling of tris(hydridosilylethyl)boranes, $B[C_2H_4–Si(CH_3)H_2]_3$, with different amounts of cyanamide, $H_2N–C\equiv N$, delivers boron-modified polysilylcarbodiimides in high yields. Due to the straight-forward synthetic procedure and the lack of by-products other than hydrogen, the Si–N (B–N) ratio in the polymers can be varied in a wide range. Ceramics are obtained by thermolysis up to 1400 °C in yields ranging from 65 to 84%. It will be published soon that the Si–B–N ratio present in **R–N1–R–N4** (R = H, Me) is maintained in their ceramics [21,22]. Apparently, the procedure described here allows for the first time to aim at the synthesis of quaternary Si–B–C–N ceramics, in which the nitrogen concentration can be adjusted as desired. This point is particularly important in that it is supposed that the extraordinary thermal stability of this type of ceramics is strongly depending on the Si–B–N ratio, i.e. the nitrogen concentration and thus the silicon nitride phase fraction, which can be calculated thermodynamically. First orienting investigations by means of high temperature TGA and X-ray diffraction (XRD) of annealed ceramics derived from the title compounds verify this assumption [22]. It will also be shown that elemental composition (and thus phase assemblage) and thermal stability can be correlated directly. Materials derived from **H–N1**, **H–N2** and **H–N3** and **Me–N1** to **Me–N5** resist thermal degradation in an Ar atmosphere up to ca. 2000 °C whereas ceramics obtained from the nitrogen-richer ceramics already decompose around 1500–1600 °C. Moreover, there are significant differences in the phase evolution of the materials at temperatures exceeding 1700–1800 °C. Nitrogen-poor ceramics resist crystallization up to at least 1800 °C whereas nitrogen-rich ceramics crystallize below 1600 °C. In the first mentioned materials, crystallization of both SiC and Si_3N_4 is observed, whereas the latter exclusively form SiC.

4. Experimental

4.1. General comments

All reactions were carried out in a purified Ar atmosphere using standard Schlenk techniques. The synthesis of tris(hydridosilylethyl)boranes $B[C_2H_4Si(R)H_2]_3$ was performed according to a procedure described in the literature [18] by a hydroboration reaction of vinylsilanes $(H_2C=CH)(R)SiH_2$ (R = H, CH_3) using a 2 M solution of $H_3B\cdot S(CH)_2$ in $C_6H_5CH_3$. Cyanamide was obtained from Sigma Aldrich and dried in a high vacuum at 25 °C for 5 h prior to its use. Tetrahydrofuran was purified by distillation from K.

Fourier-infrared spectra were obtained with a Nicolet Avatar 360 FT-IR spectrometer in KBr matrixes. Because of the insolubility of all polymers, NMR experiments were performed in the solid state. The equipment used was a Bruker MSL 300 spectrometer operating at a static magnetic field of 7.05 T (nominal ^1H frequency: 300.13 MHz). All spectra were acquired using the MAS technique with a sample rotation frequency of 5 (^{13}C, ^{29}Si) or 10–12 kHz (^1H, ^{11}B). ^1H- and ^{11}B-NMR spectra were recorded in single pulse experiments at 300.13 and 96.29 MHz, respectively. Single pulse excitation using a 45° (1.75 μs) (^{11}B) and 90° pulse (4 μs) (^1H). A recycle delay of 2 s was employed. ^{11}B chemical shifts are reported relative to $BF_3\cdot OEt_2$ (0 ppm). ^{13}C- and ^{29}Si-NMR spectra were recorded at 75.47 and 59.60 MHz, respectively, using the cross-polarization (CP) technique in which a spin lock field of 62.5 kHz and a contact time of 3 ms were applied. Typical recycle delays were 6–8 s. Chemical shifts were determined relative to external standard Q_8M_8, the trimethylsilylester of octameric silicate, and adaman

tane. These values were then expressed relative to the reference compound Me_4Si (0 ppm). Microanalysis were performed at the micro analytical department of the Max-Planck-Institut für Metallforschung Stuttgart (Germany) using a combination of different equipment (Elementar Vario EL, ELTRA CS 800 C/S Determinator, LECO TC-436 N/O Determinator) and by atom emission spectrometry (ISA JOBIN YVON JY70 Plus). TGA of the polymer-to-ceramic conversion were carried out in a flowing Ar atmosphere (50 cm^3 min^{-1}) with a Netzsch STA 409 (25–1400 °C; heating rate 5 °C min^{-1}) equipment in alumina crucibles.

4.2. Synthetic procedure

All polymers were prepared in a similar manner. A typical experiment was as follows: in a 1000 ml two-necked Schlenk flask equipped with a reflux condenser and a magnetic stirrer, 100 mmol of $B[C_2H_4Si(R)H_2]_3$ (R = H: 18.8 g; R = CH_3: 23.0 g) were dissolved in 600–800 ml of THF. After adding cyanamide (**N1**: 2.1; **N2**: 4.2; **N3**: 6.3; **N4**: 8.4; **N5**: 10.5; **N6**: 12.6 g) the mixtures were refluxed for 6 h whereby strong gas evolution was observed. Those leading to **H**–**N4**, **H**–**N5** and **H**–**N6**, **Me**–**N5**, and **Me**–**N6** gelled within 30 min. whereas precipitation of **H**–**N3**, **Me**–**N3** and **MeN4** occurred after ca. 2 h. The compounds with the lowest degree of cross-linking **H**–**N1**, **H**–**N2**, **Me**–**N1**, and **Me**–**N2** remained in solution. The mixtures were then cooled to 25 °C and the volatile parts subsequently stripped off in a high vacuum at finally 80 °C. With exception of **Me**–**N1** which is a highly viscous liquid, the obtained polymers are hard colorless solids which are insoluble in common organic solvents. All compounds, which were obtained in yields > 95% (except **H**–**N1** and **Me**–**N1** 80%), are very sensitive towards oxidation and hydrolysis.

4.2.1. IR spectra

H–**N1**: ν(N–H) 3374 w, ν(C–H) 2945 m, 2903 m, 2869 m, ν_a(NCN) 2202 s, ν(Si–H) 2149 s, δ_a(C–CH_3) 1459 m, ν(C–C) 1155 m, δ(SiH_3) 922 m.

H–**N2**: ν(N–H) 3383 s, ν(C–H) 2925 m, 2863 m, ν_a(NCN) 2208 s, ν(Si–H) 2155 s, ν(C=N) 1641 m, δ_a(C–CH_3) 1459 w, δ_s(C–CH_3) 1396 w, ν(C–C) 1155 m, δ_s(SiH_3) 922 w.

H–**N3**: ν(N–H) 3379 s, ν(C–H) 2927 m, 2867 m, ν_a(NCN) 2211 vs, ν(Si–H) 2151 vs, ν(C=N) 1637 m, δ_a(C–CH_3) 1458 w, δ_s(C–CH_3) 1384 w, ν(C–C) 1154 m, δ_s(SiH_3) 920 w.

H–**N3.5**: ν(N–H) 3372 s, ν(C–H) 2933 m, 2903 m, 2868 m, ν(Si–H) 2138 vs, ν(C=N) 1637 m, δ_a(C–CH_3) 1455 m, δ_s(C–CH_3) 1397 m, ν(C–C) 1155 s, δ(CH_3) 938 s.

H–**N4**: ν(N–H) 3373 s, ν(C–H) 2934 m, 2867 m, ν_a(NCN) 2211 vs, ν(Si–H) 2153 vs, ν(C=N) 1640 m, δ_a(C–CH_3) 1459 w, δ_s(C–CH_3) 1397 w, ν(C–C) 1155 m, δ(CH_3), δ(SiH_3) 923 w.

H–**N5**: ν(N–H) 3364 s, ν(C–H) 2929 m, 2902 m, 2865 m, ν_a(NCN) 2208 vs, ν(Si–H) 2147 vs, ν(C=N) 1640 m, δ_a(C–CH_3) 1455 w, δ_s(C–CH_3) 1397 w, ν(C–C) 1156 m, δ(CH_3) 940 m, δ(SiH_3) 924 w.

H–**N6**: ν(N–H) 3387 s, ν(C–H) 2930 m, 2864 m, ν_a(NCN) 2208 s, ν(Si–H) 2147 vs, ν(C=N) 1637 m, δ_a(C–CH_3) 1459 w, δ_s(C–CH_3) 1396 w, ν(C–C) 1155 m.

Me–**N1**: ν(C–H) 2960 m, 2906 m, 2871 m, ν(Si–H) 2130 vs, ν(C=N) 1638 w, δ_a(C–CH_3) 1461 w, δ_s(C–CH_3) 1396 w, δ_s(Si–CH_3) 1253 m, ν(C–C) 1156 w, δ_a(CBC) 1077 m, δ(SiH_2) 947 s, δ(SiH_2) 888 vs, ν(SiC) 761 s.

Me–**N2**: ν(N–H) 3394 m, ν(C–H) 2960 m, 2903 m, 2869 m, ν_a(NCN) 2202 s, ν(Si–H) 2129 s, ν(C=N) 1639 m, δ_a(C–CH_3) 1461 w, δ_s(C–CH_3) 1399 w, δ_s(Si–CH_3) 1253 m, ν(C–C) 1155 m, δ_a(CBC) 1087 m, δ(SiH_2) 947 m, δ(SiH_2) 889 s.

Me–**N3**: ν(N–H) 3377 m, ν(C–H) 2957 m, 2903 m, 2869 m, ν_a(NCN) 2207 vs, ν(Si–H) 2129 vs, ν(C=N) 1614 m, δ_a(C–CH_3) 1455 w, δ_s(C–CH_3) 1404 w, δ_s(Si–CH_3) 1254 m, ν(C–C) 1156 m, δ(SiH_2) 889 m, ν(SiC) 781 m.

Me–**N3.5**: ν(N–H) 3380 m, ν(C–H) 2957 m, 2901 m, 2869 m, ν(NCN) 2205 vs, ν(C=N) 1642 m, δ_a(C–CH_3) 1458 w, δ_s(C–CH_3) 1397 w, δ_s(Si–CH_3) 1255 m, ν(C–C) 1155 m, δ_a(CBC) 1084 m, δ(SiH_2) 947 m, γ(SiH_2) 889 s, δ(SiC) 782 s.

Me–**N4**: ν(N–H) 3397 s, ν(C–H) 2956 m, 2902 m, 2868 m, ν_a(NCN) 2207 vs, ν(Si–H) 2173 vs, ν(C=N) 1638 s, δ_a(C–CH_3) 1461 m, δ_s(C–CH_3) 1401 m, δ_s(Si–CH_3) 1256 s, ν(C–C) 1157 s.

Me–**N5**: ν(N–H) 3345 s, ν(C–H) 2956 m, 2923 m, 2870 m, ν_a(NCN) 2208 vs, ν(C=N) 1638 m, δ_a(C–CH_3) 1460 m, δ_s(C–CH_3) 1399 m, δ_s(Si–CH_3) 1255 s, ν(C–C) 1154 m,.

Me–**N6**: ν(N–H) 3338 s, ν(C–H) 2950 m, 2919 m, 2862 m, ν_a(NCN) 2203 vs, ν(C=N) 1637 m, δ_a(C–CH_3) 1459 m, δ_s(C–CH_3) 1398 m, δ_s(Si–CH_3) 1256 m, ν(C–C) 1154 m, ν(SiC) 780 s.

4.2.2. NMR spectra

Chemical shift values are reported in ppm relative to Me_4Si (^1H, ^{13}C, ^{29}Si; $\delta = 0$) or $BF_3 \cdot OEt_2$ (^{11}B; $\delta = 0$). Solid state NMR spectra were obtained by MAS-NMR with (^{13}C, ^{29}Si) or without CP. All resonance signals appear broadened. NMR spectra of **Me**–**N1** were recorded in C_6D_6 solution.

H–**N2**: ^{11}B: 0.0 (BC_3N); ^{29}Si: −17.0, −30.0 ($CSiH_2N$), −55.0 ($CSiH_3$); ^{13}C: 160.0 (C=N), 130.0 (N=C=N), 10.0 (C_2H_4).

H–**N3**: ^1H: 5.0 (SiH), 2.0 (CH); ^{11}B: −5.0 (BC_3N); ^{29}Si: −25.0 ($CSiH_2N$), −55.0 ($CSiH_3$); ^{13}C: 160.0 (C=N), 130.0 (N=C=N), 10.0 (C_2H_4).

H–N4: ^{11}B: −10.0 (BC_3N); ^{29}Si: −30.0 ($CSiH_2N$, $CSiHN_2$); ^{13}C: 160.0 (C=N), 130.0 (N=C=N), 10 (C_2H_4).

H–N5: ^{11}B: −10.0 (BC_3N); ^{29}Si: −30.0 ($CSiHN_2$); ^{13}C: 160.0 (C=N), 130.0 (N=C=N), 10.0 (C_2H_4).

H–N6: ^{1}H: 4.2 (SiH), 2.5 (CH); ^{29}Si: −30.0 ($CSiHN_2$); ^{13}C: 160.0 (C=N), 125.0 (N=C=N), 10.0 (C_2H_4).

Me–N1 (recorded in C_6D_6 solution) ^{1}H: 4.0 (m, SiH), 1.6 (m $CHCH_3$, BCH_2), 0.6 (m, $SiCH_2$), 0.2 (m, $SiCH_3$); ^{11}B{^{1}H}: 82.8 (BC_3), −2.7 (BC_3N); ^{29}Si{^{1}H}: −28.5–−32.9; ^{13}C{^{1}H}: 122.7 (N=C=N), 17.0–22.0 (m, $CHCH_3$, BCH_2), 9.0–14.0 (m, $CHCH_3$), 3.0–6.0 (m, $SiCH_2$), −10.0 (m, $SiCH_3$).

Me–N2: ^{11}B: 0.0 (BC_3N); ^{29}Si: −2.0 (C_2SiN_2), −12.0 (C_2SiNH), −33.0 (C_2SiH_2); ^{13}C: 165.0 (C=N), 130.0 (N=C=N), 10.0 (C_2H_4), 0.0 ($SiCH_3$).

Me–N3: ^{1}H: 5.0 (Si–H), 2.0 (C_2H_4); ^{11}B: −15.0 (BC_3N); ^{29}Si: 0.0 (C_2SiN_2), −10.0 (C_2SiNH), −30.0 (C_2SiH_2); ^{13}C: 165.0 (C=N), 130.0 (N=C=N), 10.0 (C_2H_4), 0.0 ($SiCH_3$).

Me–N4: ^{11}B: −7.0 (BC_3N); ^{29}Si: −5.0 (C_2SiN_2), −15.0 (C_2SiNH); ^{13}C: 165.0 (C=N), 130.0 (N=C=N), 10.0 (C_2H_4), 0.0 ($SiCH_3$).

Me–N6: ^{1}H: 1.5 (CH); ^{11}B: −10 (BC_3N); ^{29}Si: −5 (C_2SiN_2).

Acknowledgements

The authors would like to thank Gerhard Kaiser for performing elemental analysis and Sabine Nast for her encouraging co-operation in the polymer synthesis. Thanks also to C. Fasel (TU Darmstadt) for recording TGA-MS. Deutsche Forschungsgemeinschaft (DFG) is acknowledged for financial support.

References

[1] (a) D. Seyferth, H. Plenio, J. Am. Ceram. Soc. 73 (1990) 2131;
(b) D. Seyferth, H. Plenio, W.S. Rees, Jr., K. Büchner, Silicon Ceramics with a Dash of Boron in Frontiers of Organosilicon Chemistry, The Royal Society of Chemistry, Cambridge, 1991, p. 15.

[2] (a) Y.D. Blum, R.M. Laine, US Pat. 4,801,439 (1989);
(b) Y.D. Blum, R.M. Laine, US Pat. 5,017,529 (1991).

[3] (a) M. Jansen, H.-P. Baldus, Ger. Offen. DE 410 71 08 A1, 1992;
(b) H.-P. Baldus, O. Wagner, M. Jansen, Mat. Res. Soc. Symp. Proc. 271 (1992) 821;
(c) H.-P. Baldus, M. Jansen, O. Wagner, Key Eng. Mater. 89–91 (1994) 75;
(d) H.-P. Baldus, M. Jansen, Angew. Chem. 109 (1997) 338;
(e) H.-P. Baldus, M. Jansen, Angew. Chem. Int. Ed. Engl. 36 (1997) 328.

[4] (a) A. Kienzle, PhD Thesis, Universität Stuttgart, 1994;
(b) R. Riedel, A. Kienzle, W. Dressler, L. Ruwisch, J. Bill, F. Aldinger, Nature 382 (1996) 796;
(c) R. Riedel, J. Bill, A. Kienzle, Appl. Organomet. Chem. 10 (1996) 241.

[5] (a) K. Su, E.E. Remsen, G.A. Zank, L.G. Sneddon, Chem. Mater. 5 (1993) 547;
(b) K. Su, E.E. Remsen, G.A. Zank, L.G. Sneddon, Polym. Prep. 34 (1993) 334;
(c) T. Wideman, K. Su, E.E. Remsen, G.A. Zank, L.G. Sneddon, Chem. Mater. 7 (1995) 2203;
(d) P.J. Fazon, E.E. Remsen, J.S. Beck, P.J. Carroll, A.R. McGhie, L.G. Sneddon, Chem. Mater. 7 (1995) 1942;
(e) T. Wideman, K. Su, E.E. Remsen, G.A. Zank, L.G. Sneddon, Mat. Res. Soc. Symp. Proc. 410 (1996) 185;
(f) T. Wideman, E. Cortez, E.E. Remsen, G.A. Zank, P.J. Carroll, L.G. Sneddon, Chem. Mater. 9 (1997) 2218.

[6] D. Srivastava, E.N. Duesler, R.T. Paine, Eur. J. Inorg. Chem. (1998) 855.

[7] (a) M. Weinmann, J. Schuhmacher, H. Kummer, S. Prinz, J. Peng, H.J. Seifert, M. Christ, K. Müller, J. Bill, F. Aldinger, Chem. Mater. 12 (2000) 623;
(b) A. Müller, P. Gerstel, M. Weinmann, J. Bill, F. Aldinger, J. Europ. Ceram. Soc. 20 (2000) 2655;
(c) M. Weinmann, in: J. Bill, F. Wakai, F. Aldinger (Eds.), Precursor-Derived Ceramics, Wiley-VCH, Weinheim, 1999, p. 83;
(d) M. Weinmann, J. Bill, F. Aldinger, Ger. Offen. DE 197 41 458 A1, 1999;
(e) F. Aldinger, M. Weinmann, J. Bill, Pure Appl. Chem. 70 (1998) 439;
(f) J. Bill, F. Aldinger, Adv. Mater. 7 (1995) 775.

[8] (a) M. Weinmann, R. Haug, J. Bill, F. Aldinger, J. Schuhmacher, K. Müller, J. Organomet. Chem. 541 (1997) 345;
(b) M. Weinmann, R. Haug, J. Bill, M. De Guire, F. Aldinger, Appl. Organomet. Chem. 12 (1998) 725.

[9] (a) M. Weinmann, T.W. Kamphowe, J. Schuhmacher, K. Müller, F. Aldinger, Chem. Mater. 12 (2000) 2112;
(b) M. Weinmann, T.W. Kamphowe, J. Bill, F. Aldinger, Ger. Offen. DE. 197 41 460 A 1, 1999.

[10] A. Kienzle, A. Obermeyer, R. Riedel, F. Aldinger, A. Simon, Chem. Ber. 126 (1993) 2569.

[11] (a) P.R. Jones, J.K. Myers, J. Organomet. Chem. 34 (1972) C9;
(b) L.M. Ruwisch, P. Dürichen, R. Riedel, Polyhedron 19 (2000) 323.

[12] R. Haug, M. Weinmann, J. Bill, F. Aldinger, J. Europ. Ceram. Soc. 19 (1999) 1.

[13] For recent reviews on thermolysis of polysilazanes see: (a) R.M. Laine, A. Sellinger, Si-containing ceramic precursors, in: Z. Rappoport, Y. Apeloig (Eds.), The Chemistry of Organic Silicon Compounds, vol. 2, John Wiley & Sons, London, 1998;
(b) E. Kroke, Y.-L. Li, C. Konetschny, E. Lecomte, C. Fasel, R. Riedel, Mater. Sci. Eng. R26 (2000) 97.

[14] H.J. Seifert, J. Peng, H.L. Lukas, F. Aldinger, J. Alloys Comp. 320 (2001) 251 and literature cited therein, in press.

[15] (a) Calphad: Calculation of Phase Diagrams, see also corresponding Journal. Calculations in the Si–B–C–N system are in detail described in: (a) B. Kasper, PhD thesis, Universität Stuttgart, 1996;
(b) H.J. Seifert, F. Aldinger, Z. Metallkd. 87 (1996) 841.

[16] (a) E.A. Ebsworth, M.J. Mays, Angew. Chem. 74 (1962) 117;
(b) J. Pump, E. Rochow, Z. Anorg. Allg. Chem. 330 (1964) 101.

[17] (a) R. Riedel, A.O. Gabriel, Adv. Mater. 11 (1999) 207;
(b) A.O. Gabriel, R. Riedel, Angew. Chem. Int. Ed. Engl. 36 (1997) 384;
(c) A.O. Gabriel, R. Riedel, Proc. 21st Annual Cocoa Beach

Conference and Exposition, The American Ceramic Society 1997, ISSN 0196-6219, FL, USA 18 (1997) 713.
[18] M. Weinmann, T.W. Kamphowe, P. Fischer, F. Aldinger, J. Organomet. Chem. 592 (1999) 115.
[19] M. Weinmann, S. Nast, F. Berger, K. Müller, F. Aldinger, Appl. Organomet. Chem. 15 (2001) 867.
[20] A.O. Gabriel, R. Riedel, S. Storck, W.F. Maier, Appl. Organomet. Chem. 11 (1997) 833.
[21] M. Hörz, F. Berger, K. Müller, F. Aldinger, M. Weinmann, unpublished.
[22] M. Hörz, Diploma Thesis, University of Stuttgart, 2001.